X-645-70-399
PREPRINT

NASA TM X-65378

MAGNETOPAUSE ATTITUDES DURING OGO-5 CROSSINGS

B. G. LEDLEY

OCTOBER 1970

GSFC

GODDARD SPACE FLIGHT CENTER
GREENBELT, MARYLAND

MAGNETOPAUSE ATTITUDES DURING OGO-5 CROSSINGS

by

B. G. Ledley

October 1970

Goddard Space Flight Center
Greenbelt, Maryland 20771

Introduction

The technique for determining the attitude of the magnetopause current layer which was introduced by Sonnerup and Cahill [1967] has been applied by several experimenters (Sonnerup and Cahill [1967, 1968], Cummings and Coleman [1968], Kauffman and Konradi [1969], Aubry et al. [1970]). However, the only surveys extending over large areas of the magnetopause have used data from Explorer 12, which provides measurements of the magnetic field components with a resolution of 24 gammas. The satellite's spin improved the effective resolution in the spin plane; nevertheless, it appears desirable to further apply the technique to data with higher measurement resolution. This paper reports the study of magnetopause crossings of the Fifth Orbiting Geophysical Observatory (OGO-5), using data taken by the Goddard Space Flight Center magnetic field experiment which measures field components with a resolution of 1/4 gamma. The sampling rate of the three components is 1.7, 14, or 56 samples per second, depending on the mode of operation of the observatory. A total of 70 crossings were examined, of which 31 satisfied accuracy criteria of the calculation. These crossings were located at subsatellite local times between 1020 and 0430, and solar magnetospheric latitudes between -7° and $+40^{\circ}$.

Application of the Technique

The technique of Sonnerup and Cahill consists of determining the components of a unit vector $\hat{n}_1$ which will minimize the variance

$$\sigma_1{}^2 = \frac{1}{N}\sum_{i=1}^{N} [\vec{B}_i \cdot \hat{n}_1 - \bar{\vec{B}} \cdot \hat{n}_1]^2$$

where $\vec{B}_i$ represents one of N individual field measurements taken during a magnetopause crossing. The quantity $\bar{\vec{B}}$ is equal to $\frac{1}{N}\sum_{i=1}^{N} \vec{B}_i$

$\hat{n}_1$ is interpreted to be the normal to the magnetopause current layer. This computation, of minimization of the variance, is equivalent to that of finding the smallest principal axis of the variance ellipsoid defined by Equation [1]. The calculation also yields $\hat{n}_2$ and $\hat{n}_3$, and σ_2 and σ_3, the directions and magnitudes of the other two principal axes.

Each OGO-5 crossing was analyzed as follows: The approximate time of crossing of the center of the current layer was determined by inspection. The measurements were then grouped in a series of intervals each centered on this time and having a successively increasing width (see Figure 1). The increment of data for each successive segment, and the largest interval of data used were chosen for each crossing so that the innermost segments would contain only measurements taken inside the current layer, and the outermost would contain, in addition, magnetospheric and magnetosheath measurements. (By "inside the current layer", one means within a time interval when the field can be recognized as being transitional between the magnetospheric field and the magnetosheath field.)

Typically, about one minute of data and ten or more nested segments were used. The three vectors $\hat{n}_1$, $\hat{n}_2$, and $\hat{n}_3$ and their corresponding variances were determined for each segment. In practice, it was usually found that the direction of $\hat{n}_1$, $\hat{n}_2$, and $\hat{n}_3$ for the inner segments varied considerably from one segment to another. As the segment width increased, a series of segments were commonly obtained which had relatively constant directions of $\hat{n}_1$. As still wider segments were used, the variance would increase and the direction of $\hat{n}_1$ might again vary. The criterion adopted for an acceptable determination of $\hat{n}_1$ was that there be a consecutive set of segments, greater in number than those in the variable inner region, for which (1) the directions of $\hat{n}_1$ all fell within a cone of total angle less than 15°; (2) the magnitude of σ_1 was less than 0.3 times the magnitude of the vector change in the field across the magnetopause current layer; and, (3) σ_2/σ_1 was $< 1/3$. When these conditions were satisified, a representative value of $\hat{n}_1$ was chosen from one of the acceptable segments.

In fact, the average total cone angle for the 31 acceptable crossings was 6°. The data rate varied from 1.7 to 56 samples per second depending on the mode of operation of the observatory, but trial calculations showed that the calculation was insensitive to both the sampling rate and the exact time chosen for the center of the nested segments. The magnetopause crossings were found by scanning only the magnetic field experiment data; a relatively clear identification was required before an event was chosen for calculation.

The $\hat{n}_i$ vectors were transformed into a spherical system, in which the polar axis is the earth-to-sun line and the zero direction fot the azimuthal angle is a line perpendicular to a plane containing the earth-sun line and the magnetic dipole axis of the earth (See Figure 2).

A simple model surface, suggested by Mead (private communication) was used to generate theoretical normal vectors at the coordinates of the magnetopause crossings. The model has a geocentric radial distance proportional to sec $\theta/2$ where θ is the angle from the polar axis and is a surface of revolution about this axis. This surface flares out with increasing θ slightly more than does the published Mead and Beard model [1964]. For example, the ratio of the radial distance of $\theta = 90^{\circ}$ to that at $\theta = 0^{\circ}$ is 4% greater in this than in the published Mead and Beard model [op. cit.]. This general behavior is in accordance with experimental observations of magnetopause locations.

Results

(1) Deflection of the Current Layer

Figure 3 is a plot of $\Delta\theta$ versus θ for each acceptable calculation of $\hat{n}_1$. Here $\Delta\theta$ is the angle θ of the experimentally determined $\hat{n}_1$ vector minus the angle θ of the $\hat{n}_1$ vector obtained from the simple model. The abscissa, θ, is the θ coordinate of the satellite position at the crossing. In general, $\Delta\theta$ is seen to be greater for the magnetosheath-to-magnetosphere crossings than for the magnetosphere-to-magnetosheath crossings.

Figure 3 is a plot of n_ϕ versus ϕ, where n_ϕ is the component of the experimentally determined unit vector $\hat{n}_1$ perpendicular to the plane of constant ϕ passing through the satellite position. The abscissa is the ϕ coordinate of the satellite position at the crossing. The value of n_ϕ from the simple model would be zero everywhere, since the model is a surface of revolution about the polar axis. In this plot a positive value of n_ϕ corresponds to the direction of increasing angle ϕ. The plot symbols have the same meaning as before.

It will be noted that in this plot the two directions of crossing are not clearly separated as they were in Figure 2. This tendency for the normal vector to be deflected to a larger or smaller value of θ, depending on whether the crossing is from the magnetosphere to the transition region or vice versa is consistent with a model in which the crossing occurs as the result of a propagation of a compression or expansion front over the surface of the magnetosphere from the day to the night side. This model was suggested, for example, by Kauffman and Konradi (op. cit.) in their interpretation of Explorer 12 results. Aubry et al. (op. cit.), also interpret their data to signify anti-solar propagating waves. If this model is applicable, then it appears that a large majority of the present crossings must have occurred during the passage of such fronts past the satellite.

The dotted lines in Figure 3 are least-squares fits to the two directions of crossing. The equations to the least square lines are: $\Delta\theta = 17.7 - (0.21 \pm 0.15)\theta$ for transition region to magnetosphere crossings, and $\Delta\theta = -19.9 - (0.09 \pm 0.17)\theta$ for magnetosphere to transition region crossings. The units are degrees. The errors quoted for the slope are standard deviations, calculated under the assumption that a linear relationship exists between $\Delta\theta$ and θ for each type of crossing. These two lines converge slightly with increasing θ, but the convergence is not statistically significant. That is, to the accuracy of these data, there is no evidence of either an increase or a decrease of the deflection of the normal vector with increasing sun-earth-satellite angle, θ.

(2) <u>Magnitude of the Field Perpendicular to the Current Layer</u>

In reconnection models of the magnetosphere, the magnitude of the magnetic field perpendicular to the magnetopause current layer is a measure of the reconnection rate, e.g. Levy et al. [1964]. In these models reconnection can only occur between the magnetospheric and magnetosheath fields when they are inclined at an angle of greater than 90° with respect to each other and then the perpendicular field will be inward directed in the Northern Hemisphere and outward in the Southern Hemisphere. Levy et al. [op. cit.] predict that this perpendicular field will be 10-20% of the adjacent magnetospheric and magnetosheath fields when these latter fields are anti-parallel. When the magnetospheric and magnetosheath fields make an angle of less than 90°, the perpendicular component is predicted to be small or zero.

An attempt was made to test this model by using the 31 OGO-5 calculations of magnetopause attitude. First, the angle between the transition region and magnetopsheric fields was determined by examining the data taken within one or two minutes on either side of the magnetopause. The determination of this angle was, in many crossings, impossible on account of rapid direction changes in the transition region field. Of the 31 crossings, 17 were judged to be sufficiently stable to define whether the angle was greater or less than 90° (see Table 1). Ten were greater than 90°; they were all in the Northern Solar Magnetospheric Hemisphere. Seven were less than 90°; six of these were in the Northern Solar Magnetospheric Hemisphere, and one in the Southern Hemisphere.

For each of the 17 crossings, the ratio of the normal component to the total magnetospheric field was computed, viz. $(\bar{\vec{B}} \cdot \hat{n}_1)/B_M$ where B_M is the magnitude of the magnetospheric field adjacent to the to the magnetopause and the average $\bar{\vec{B}} \cdot \hat{n}_1$ was taken over the segment of data used to determine $\hat{n}_1$. A standard deviation σ_1/B_M was also computed for each ratio where σ_1, defined in Equation 1, was obtained from the same segment of data. The average of the ratios $(\bar{B} \cdot \hat{n}_1)/B_M$ for the ten crossings with fields at greater than 90^o was $-0.03_4 \pm.09$, and for the seven cases where the fields were at less than 90^o, the ratio was $-0.05_3 \pm.06$. Here, a negative sign corresponds to an inward directed field. The errors quoted are standard deviations computed from the set of ten (seven) values of the ratio $R = (\bar{B} \cdot \hat{n}_1)/B_M$ using the formula: standard deviation $= \sum_{j=1}^{N} [(R_j - \bar{R})^2/(N - 1)]^{\frac{1}{2}}$ where R_j is the value of R for the j^{th} crossing, $\bar{R} = \sum_{j=1}^{N} (R_j/N)$ and N = 10 (or 7).

As shown in Table 1 the standard deviation σ_1/B_M of the quantity R_j for any single crossing was generally smaller than the standard deviations computed for each of the two averaged values of R; that is, there were statistically significant variations in R_j from one crossing to another; individual crossings yielded a range of values of R_j from approximately +0.1 to -0.2. Because of this variation of R_j from one crossing to another, and since both positive and negative components of the magnetic field normal to the magnetopause surface were observed when the adjacent magnetospheric and magnetosheath fields are anti-parallel, the <u>average</u> ratio, $\bar{R}$, taken over a number of crossings is not a good parameter for determining reconnection rates in this area of the magnetopause.

Conclusions

(1) The average ratio of the normal component of the magnetopause field to the adjacent magnetospheric field was 3 ± 9 percent for ten OGO-5 crossings which had occurred when the adjacent magnetospheric and transition region fields were inclined to each other at an angle of greater than 90°. The average ratio was 5 ± 6 percent for seven crossings when the fields were inclined at an angle of less than 90°. The errors quoted are largely the result of the variability of the ratio from one crossing to another. This variability precludes, in this region of the magnetosphere, the use of the average value to accurately test reconnection models that predict ratios of ten percent or less.

(2) Straight line fits to the plots of deflection of the magnetopause current layer versus the sun-earth-satellite angle for each direction of crossing show no evidence of a growth of decay of the deflection as this angle increases.

(3) The direction of these deflections is consistent with a model in which the OGO-5 crossings occur during the passage of compression or expansion fronts propagating from the day to the night side of the magnetopause. This same interpretation was first proposed by Kauffman and Konradi (op. cit.) for Explorer 12 magnetopause crossings.

ACKNOWLEDGMENTS

The assistance of H. J. Gillis, who performed the mathematical programming, is gratefully acknowledged.

REFERENCES

Aubry, Michel P., Margaret G. Kivelson, and Christopher T. Russell, Motion and Structure of the Magnetopause, Publication No. 865, Institute of Geophysics and Planetary Physics, U.C.L.A., 1970.

Cummings, W. D., and R. J. Coleman, Jr., Magnetic fields in the magnetopause and vicinity at synchronous altitude, J. Geophys. Res., 73, 5699-5718, 1968.

Kauffman, Richard L., and Andrei Konradi, Explorer 12 magnetopause observations; large scale non-uniform motion, J. Geophys. Res., 74, 3609-3627, 1969.

Levy, R. H., H. E. Petschek, and G. L. Siscoe, Aerodynamic Aspects of the Magnetospheric Flow, AIAA Journal, 2, 2065-2076, 1964.

Mead, Gilbert D., and David B. Beard, Shape of the geomagnetic field solar wind boundary, J. Geophys. Res., 69, 1169-1179, 1964.

Sonnerup, B.V.O., and L. J. Cahill, Jr., Magnetopause structure and attitude from Explorer 12 observations, J. Geophys. Res., 72, 171-183, 1967.

Sonnerup, B.V.O., and L. J. Cahill, Jr., Explorer 12 observations of the magnetopause current layer, J. Geophys. Res., 73, 1757-1770, 1968.

FIGURE CAPTIONS

FIGURE 1. N segments of successively increasing width, centered on the magnetopause current layer.

FIGURE 2. The geocentric spherical coordinate system used. The polar axis points to the sun; the zero direction of the azimuthal angle is a line perpendicular both to this polar axis and to the geomagnetic dipole axis.

FIGURE 3. A plot of $\Delta\theta$ versus θ. $\Delta\theta$ is the difference between the θ coordinate of the experimentally determined $\hat{n}_1$ vector and the θ coordinate obtained from the simple model surface. The abscissa θ is the θ coordinate of the satellite's position. The symbol X is used for magnetosheath to magnetosphere crossings and the symbol · for magnetosphere to magnetosheath crossings.

FIGURE 4. A plot of n_ϕ, the ϕ component of the experimentally determined $\hat{n}_1$ vector, versus the ϕ coordinate of the satellite's position. Note that the simple model surface would predict that n_ϕ would be zero everywhere. The plot symbols have the same meaning as in Figure 3.

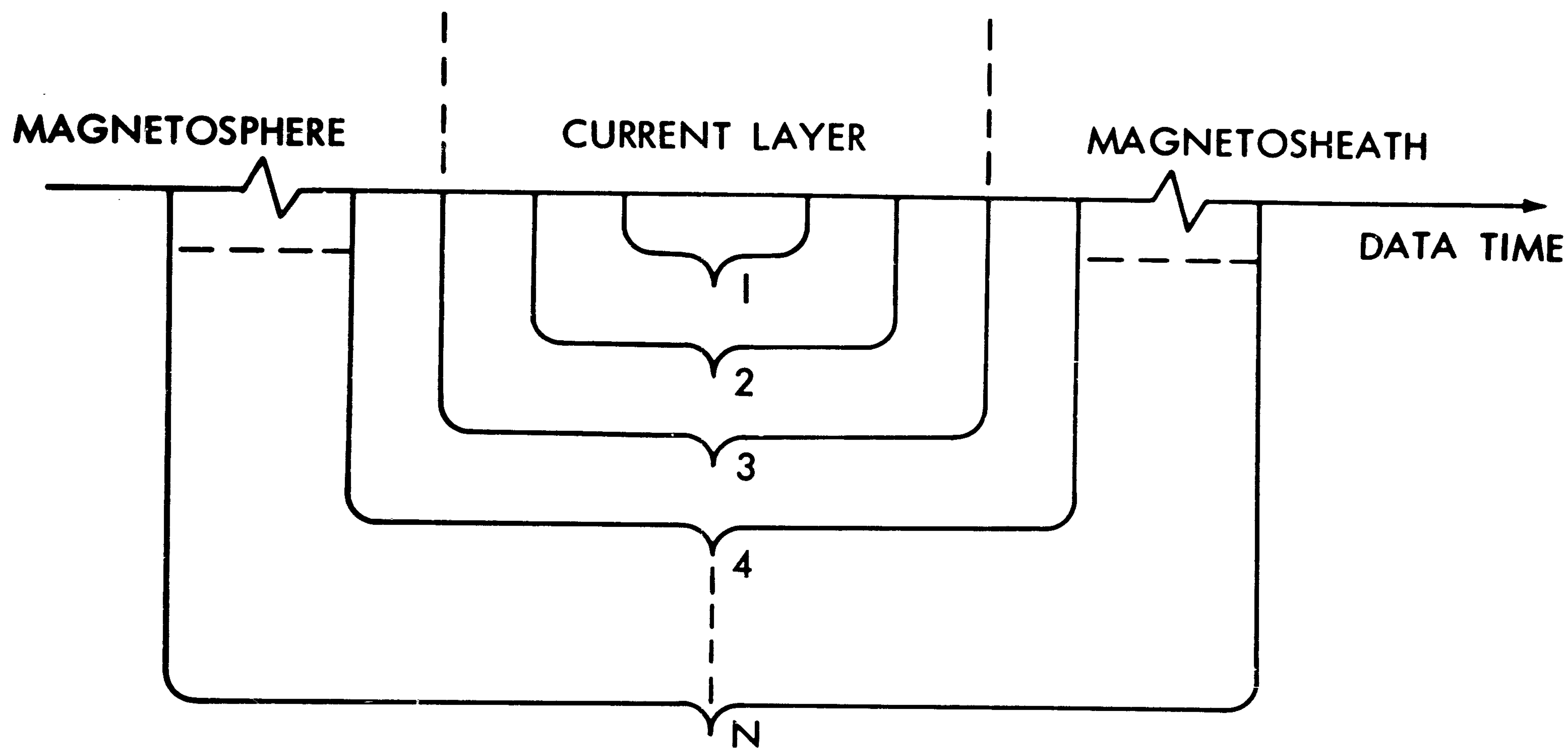
MAGNETOSPHERE
CURRENT LAYER
MAGNETOSHEATH
DATA TIME
1
2
3
4
N

FIG 1

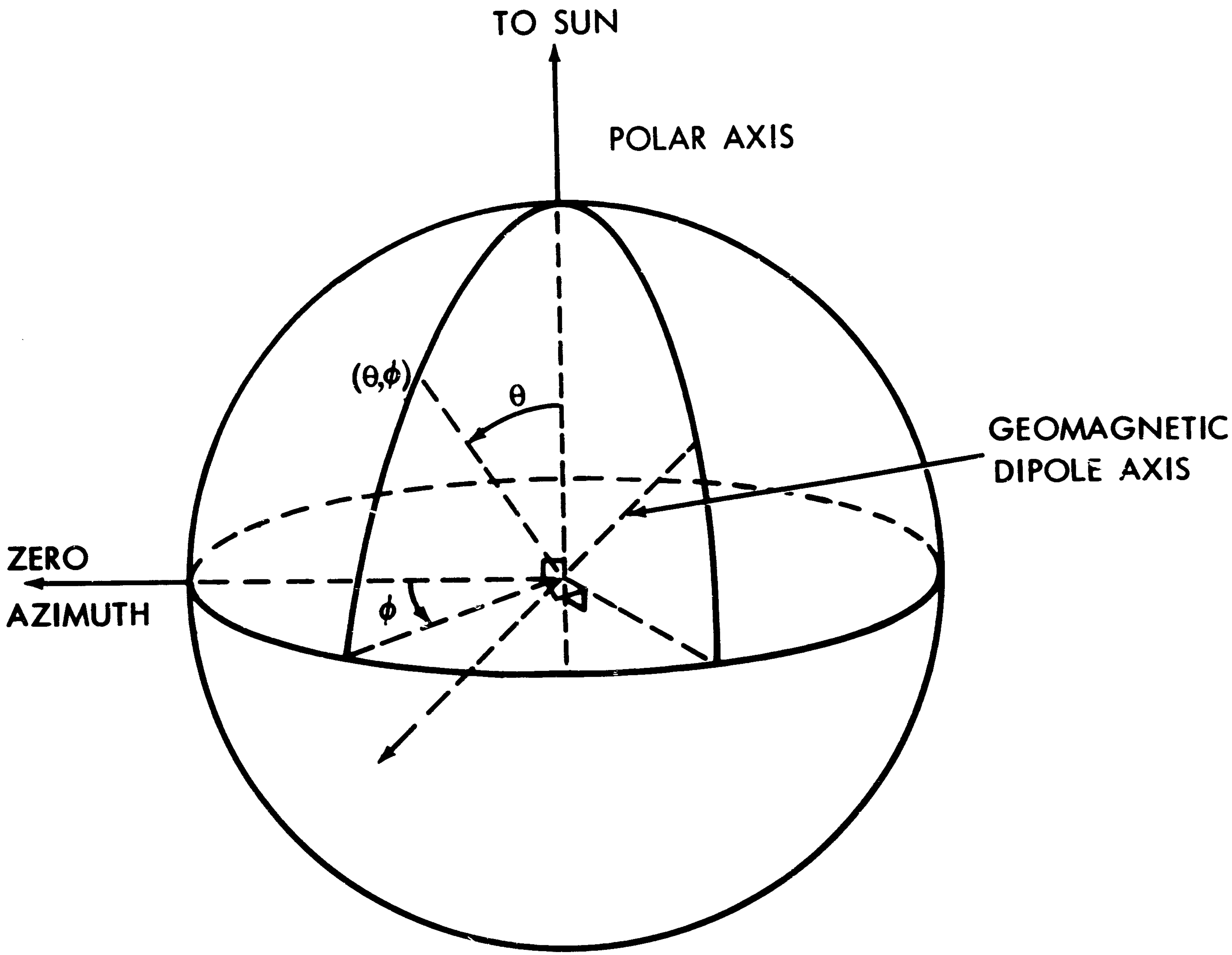
TO SUN
POLAR AXIS
(θ,φ)
θ
GEOMAGNETIC
DIPOLE AXIS
ZERO
AZIMUTH
φ

FIG 2

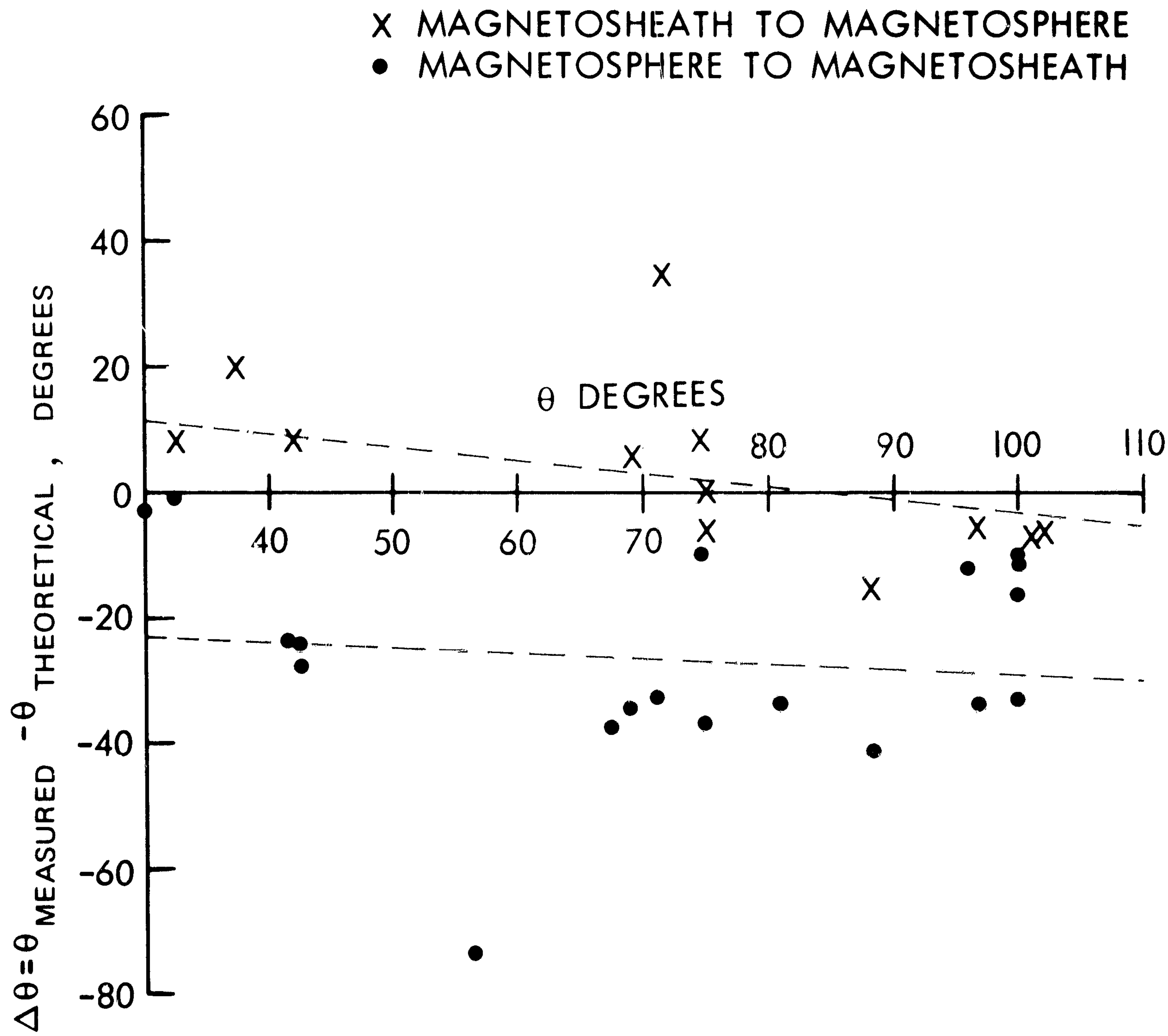
X MAGNETOSHEATH TO MAGNETOSPHERE
• MAGNETOSPHERE TO MAGNETOSHEATH
Δθ=θ MEASURED -θ THEORETICAL , DEGREES
θ DEGREES
60
40
20
0
-20
-40
-60
-80
40
50
60
70
80
90
100
110

FIG 3

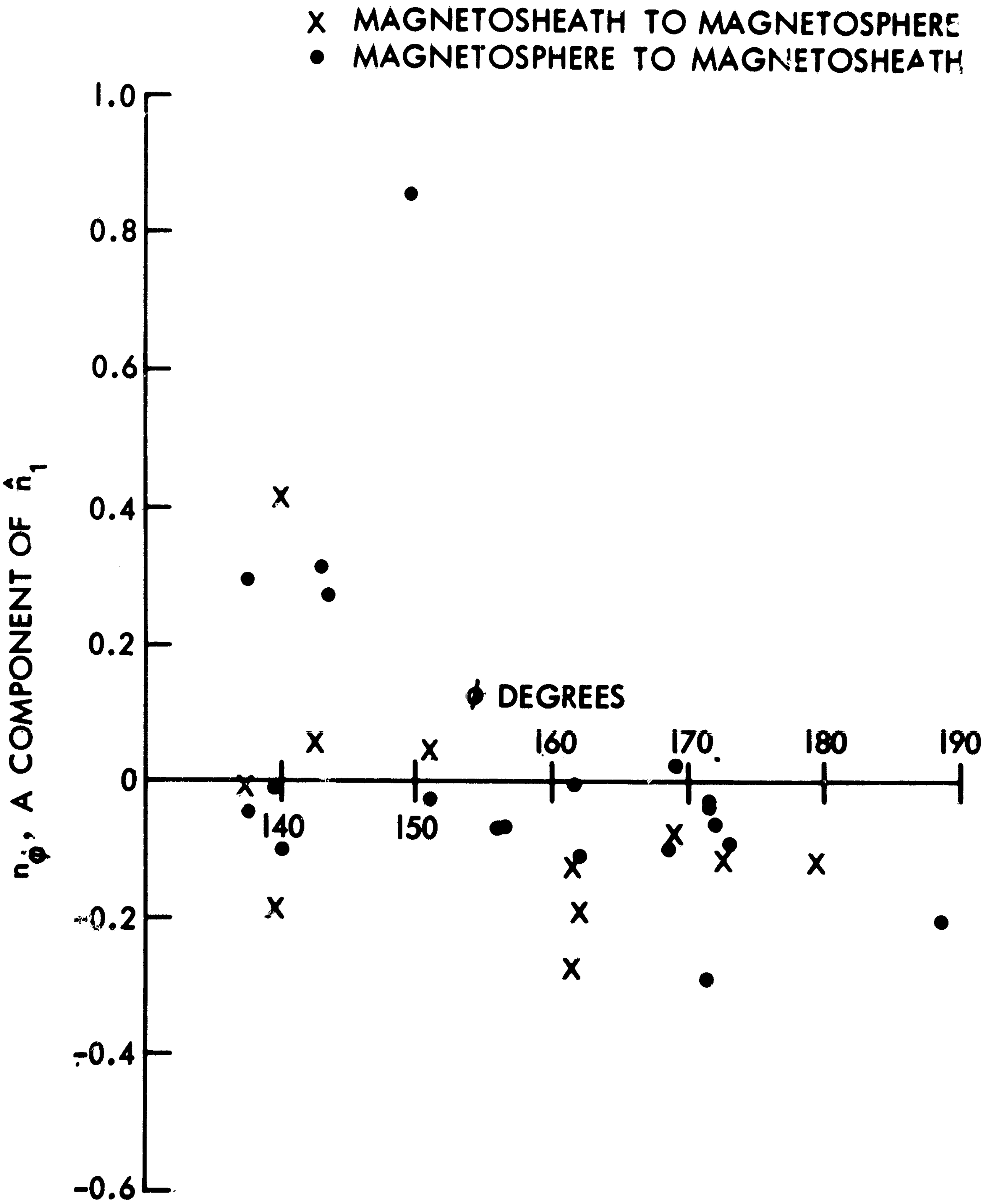

X MAGNETOSHEATH TO MAGNETOSPHERE
• MAGNETOSPHERE TO MAGNETOSHEATH
1.0
0.8
0.6
0.4
0.2
0
-0.2
-0.4
-0.6
$n_{\hat{\phi}}$, A COMPONENT OF $\hat{n}_1$
φ DEGREES
140
150
160
170
180
190

FIG 4

TABLES

TABLE 1. The 31 acceptable calculations are summarized here. A +ve sign in the column $(\vec{B} \cdot \hat{n}_1)/B_M$ denotes an outward directed normal component. The column headed "subtended angle" refers to the angle between the magnetospheric and magnetosheath fields adjacent to the magnetopause.

TABLE 1: Summary of Calculations

Time of Crossing (1968) Day	Hr	Min	Sec	Coordinates: Geocentric Distance (1000 km units)	θ (deg.)	φ (deg.)	Δθ (deg.)	n_ϕ	$\frac{\vec{B} \cdot \hat{n}_1}{B_M}$	$\frac{\sigma_1}{B_M}$	Direction of Crossing	Subtended Angle (degrees)
66	21	44	13	82	30°	156.5°	-3°	-.066	+.043	.04	M → T	>90°
70	02	22	30	87	100	156	-10	-.068	-.105	.07	M → T	>90
77	08	51	6	70	32.5	151	-1.5	-.023	-.043	.03	M → T	?
77	08	51	59	70	32.5	151	+8.5	+.046	-.049	.04	T → M	?
80	10	39	12	76	86	139.5	-34	-.003	+.016	.01	M → T	<90
87	17	43	20	77	42.5	171.5	-24.5	-.037	+.122	.05	M → T	>90
87	17	44	55	77	42	171.5	+8	-.115	-.012	.04	T → M	>90
87	17	46	58	77	42	172	-27.5	-.289	-.009	.03	M → T	?
87	17	56	46	75	41.5	173	-22	-.090	+.009	.05	M → T	>90
87	19	05	18	64	37.5	179.5	+20.5	-.115	-.054	.05	T → M	?
93	13	36	25	95	88.5	143.5	-41.5	+.272	+.136	.08	M → T	?
93	13	50	52	97	88	140	-15	+.419	-.016	.04	T → M	?
105	22	58	48	73	56.5	188.5	-74	-.203	-.062	.02	M → T	<90
106	13	47	55	96	96.5	142.5	-5.5	+.058	-.032	.04	T → M	<90
106	13	59	25	97	96	143	-12.5	+.314	-.058	.04	M → T	<90

TABLE 1: <u>Summary of Calculations</u>
(continued)

Time of Crossing (1968) Day	Hr	Min	Sec	Coordinates: Geocentric Distance (1000 km units)	θ (deg.)	φ (deg.)	Δθ (deg.)	n_ϕ	$\frac{\vec{B} \cdot \hat{n}_1}{B_M}$	$\frac{\sigma_1}{B_M}$	Direction of Crossing	Subtended Angle (degrees)
109	04	49	39	100	97°	149.5°	-34°	+.856	-.168	.05	M → T	<90°
114	09	12	45	97	101	137.5	-7	-.004	-.057	.03	T → M	<90
114	09	48	22	101	100	137.5	-12	-.046	-.069	.04	M → T	?
114	10	01	00	102	100	137.5	-33.5	+.297	+.047	.04	M → T	?
116	04	35	33	100	71.5	172	+34.5	-.063	-.011	.03	T → M	<90
116	05	02	35	97	71	171.5	-33	-.028	-.219	.03	M → T	>90
116	06	41	53	87	69	169	-35	+.025	-.052	.05	M → T	>90
116	06	44	56	86	69	169	+6	-.080	-.111	.03	T → M	>90
116	07	42	50	80	67.5	168.5	-37.5	-.098	-.014	.03	M → T	>90
121	10	30	58	93	75	161.5	0	-.270	+.003	.04	T → M	>90
121	10	34	12	93	75	161.5	-37	-.003	-.037	.02	M → T	?
121	10	36	40	92	75	161.5	-6	-.130	-.040	.05	T → M	?
121	10	48	08	91	74.5	162	-10	-.114	-.003	.03	M → T	?
121	10	48	55	91	74.5	162	+8.5	-.190	+.046	.04	T → M	?
122	07	42	35	114	100	140	-16.5	-.099	+.056	.07	M → T	?
122	08	19	30	117	102	139.5	-6	-.184	+.060	.07	T → M	?